

PROCEEDINGS OF SPIE

SPIDigitalLibrary.org/conference-proceedings-of-spie

Ultrafast phase imaging of propagating current flows in myelinated axons and electromagnetic pulses in dielectrics

Yide Zhang, Binglin Shen, Tong Wu, Jerry Zhao, Joseph Jing, et al.

Yide Zhang, Binglin Shen, Tong Wu, Jerry Zhao, Joseph C. Jing, Peng Wang, Kanomi Sasaki-Capela, William G. Dunphy, David Garrett, Konstantin Maslov, Weiwei Wang, Lihong V. Wang, "Ultrafast phase imaging of propagating current flows in myelinated axons and electromagnetic pulses in dielectrics," Proc. SPIE 12390, High-Speed Biomedical Imaging and Spectroscopy VIII, 1239008 (16 March 2023); doi: 10.1117/12.2653137

SPIE.

Event: SPIE BiOS, 2023, San Francisco, California, United States

Ultrafast phase imaging of propagating current flows in myelinated axons and electromagnetic pulses in dielectrics

Yide Zhang^{1†}, Binglin Shen^{1,2†}, Tong Wu^{1,3}, Jerry Zhao¹, Joseph C. Jing¹, Peng Wang¹, Kanomi Sasaki-Capela⁴, William G. Dunphy⁴, David Garrett¹, Konstantin Maslov¹, Weiwei Wang⁵, and Lihong V. Wang^{1*}

¹*Caltech Optical Imaging Laboratory, Andrew and Peggy Cherng Department of Medical Engineering, Department of Electrical Engineering, California Institute of Technology, Pasadena, CA 91125, USA*

²*Present address: Key Laboratory of Optoelectronic Devices and Systems of Guangdong Province and Ministry of Education, College of Physics and Optoelectronic Engineering, Shenzhen University, Shenzhen 518060, China*

³*Present address: Key Laboratory of Space Photoelectric Detection and Perception, Nanjing University of Aeronautics and Astronautics, Nanjing 210016, China*

⁴*Division of Biology and Biological Engineering, California Institute of Technology, Pasadena, CA 91125, USA*

⁵*Department of Biophysics, University of Texas Southwestern Medical Center, Dallas, TX 75390, USA*

† These authors contributed equally.

* Correspondence should be addressed to L.V.W. (LVW@caltech.edu).

ABSTRACT

Visualization of the spatiotemporal dynamics of propagation is fundamental to understanding dynamic processes ranging from action potentials to electromagnetic pulses, the two ultrafast processes in biology and physics, respectively. Here, we demonstrate differentially enhanced compressed ultrafast photography to directly visualize propagations of passive current flows at approximately 100 m/s along internodes from *Xenopus laevis* sciatic nerves and of electromagnetic pulses at approximately 5×10^7 m/s through lithium niobate. The spatiotemporal dynamics of both propagation processes are consistent with the results from computational models, demonstrating that our method can span these two extreme timescales while maintaining high phase sensitivity.

1. INTRODUCTION

Visualizing the spatiotemporal dynamics of propagation is fundamental to understanding processes in different areas of science and technology. Two examples are the propagation of action potentials (APs) along myelinated axons and electromagnetic pulses (EMPs) as ultrafast processes in biology and physics, respectively¹. While existing models can accurately predict their propagation speed and dynamics^{2,3}, a tool to experimentally visualize propagation may highlight characteristics unique to specific samples or materials. However, due to the extreme speed and sensitivity requirements, APs propagating along myelinated axons and EMPs propagating in dielectrics have not yet been visualized with existing imaging modalities⁴⁻⁶. Previously, we reported compressed ultrafast photography (CUP), the world's fastest camera that achieves both ultrafast imaging of up to 70 trillion frames per second (fps) and a large sequence depth of up to 1000 frames⁷⁻⁹. We also combined CUP with dark-field imaging and used pump and probe pulses to image ultrafast phase

events in transparent objects¹⁰. However, without sufficient phase sensitivity (e.g., 0.9 mrad required to measure APs in spiking HEK-293 cells⁵), our previous CUP systems were not capable of imaging either propagating APs or weak EMPs.

Here, we demonstrate differentially enhanced compressed ultrafast photography (Diff-CUP)¹¹ to directly visualize propagations of passive current flows, which plays a central role in AP propagation, at approximately 100 m/s along internodes, i.e., continuous myelinated axons between nodes of Ranvier, from *Xenopus laevis* sciatic nerves and of EMPs at approximately 5×10^7 m/s through lithium niobate (LN). Enabled by the ultrahigh speed and large sequence depth of compressed ultrafast photography and the high sensitivity of a differentially enhanced Mach-Zehnder interferometer¹², Diff-CUP can capture ultrafast phase events at 200 billion fps with a sequence depth of up to 350 frames and a phase sensitivity of 20 μ rad. The calculated conduction speeds agree with measurements by other techniques, and the spatiotemporal dynamics of these two propagation processes are consistent with the results from computational models¹³, indicating that Diff-CUP can cross these two extreme timescales while maintaining high phase sensitivity.

2. METHODS

In the Diff-CUP system (Fig. 1a)¹¹, the laser beam was split into the two arms of a Mach-Zehnder interferometer by a beamsplitter. In the sample arm, the beam passed through an LN crystal before entering the objective lens, and a glass slide on a translational stage was used to place the teased axons within the focal region of the objective lens. In the reference arm, an optical delay line was used to compensate for the optical path length difference between the two arms. The beams in the two arms were recombined using another beamsplitter and passed through the tube lens of the objectives before being directed to the streak camera in a lossless-encoding CUP setup⁸. A beamsplitter was placed before the lossless-encoding CUP setup to reflect a part of the light to an external CCD camera. A delay generator was triggered by the laser pulse signal detected by a photodiode. The triggered signal was downscaled by a delay generator to provide trigger inputs for the external CCD camera, the streak camera, a pulse generator used to induce EMPs in the LN crystal, and a stimulator used to inject passive current flows in the axons, thus enabling synchronization among all the instruments.

The single myelinated axons were dissected from a female 9+ cm *Xenopus laevis* (LM00535, Nasco) following the procedures as described in Refs. ^{14,15}. All the laboratory animal protocols were approved by the Institutional Animal Care and Use Committee of the California Institute of Technology. After euthanasia, the skin of the animal was cut to expose the biceps femoris and the intermuscular septum. The biceps femoris were separated along the intermuscular septum to expose the sciatic nerve. A nerve bundle was excised from the sciatic nerve, stored in a petri dish filled with Ringer's solution, and then transferred to an adhesion microscope slide, where the individual myelinated axons were teased out using the fine forceps and spring scissors under a phase-contrast microscope. During the procedure, more Ringer's solution was added to the dissection slide to keep the axons immersed. The dissection slide with the teased axons was then transferred to the Diff-CUP system for imaging. The slide was placed on the translational stage above the objective lens in the sample arm. After a myelinated axon with visible nodes of Ranvier was located within the field of view, a pair of parallel bipolar microelectrodes, controlled by a micromanipulator system, was placed near the axon to create field stimulation. The position of the electrodes was carefully adjusted

such that the electrode tips were immersed in Ringer's solution but not in direct contact with the axon, and the fringes in the interferogram were as wide as possible. To inject passive current flows in myelinated axons by field stimulation, an isolated pulse stimulator was used to deliver stimulating pulses with different amplitudes and pulse widths to the electrodes. The stimulator was triggered by a function generator, which was synchronized with the delay generator. If properly configured, the stimulator would inject passive current flows in the axons in every other interferogram during a Diff-CUP imaging experiment.

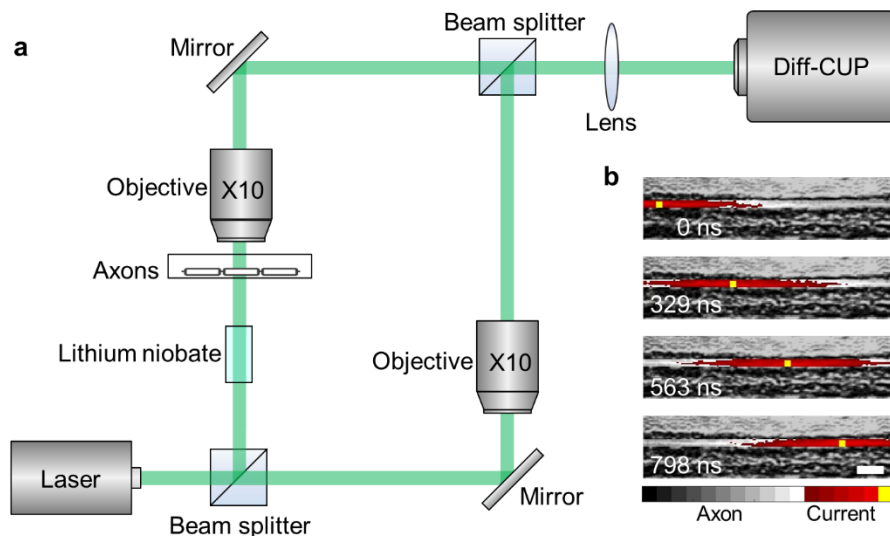


Figure 1 (a) Schematic of the Diff-CUP system. (b) Snapshots of the phase change induced by the propagating internodal current flow in a myelinated axon. Scale bar, 10 μm .

The EMPs propagating in the LN crystal imaged by the Diff-CUP system were induced by an ultra-wideband pulse generator. To induce picosecond EMPs with different amplitudes, 30-ps pulses were passed through different configurations of a monolithic amplifier, a power amplifier, and attenuators with various attenuation powers before being directed to the LN crystal. All the components in the radiofrequency pathway were matched at 50 Ω and connected using 40 GHz precision test cables with 2.92mm connectors. To avoid signal distortion and reflection due to electrical impedance mismatch, a custom-designed microstrip transmission line was fabricated to deliver the EMPs to the LN crystal. The microstrip line and the LN crystal were connected via a 135° mitered bend to further reduce the reflection of the EMPs from the boundary. The pulse generator, triggered by the delay generator, would induce EMPs in the LN crystal in alternating interferograms during a Diff-CUP imaging experiment.

3. RESULTS

Combined with a differential approach and a suitable field of view, Diff-CUP achieves a phase sensitivity of 20 μrad , the greatest phase sensitivity reported to date by an ultrafast imaging approach. Diff-CUP directly visualizes propagations of passive current flows, which play a central role in AP propagation, along internodes, i.e., continuous myelinated axons between nodes of Ranvier, from *Xenopus laevis* sciatic nerves (Fig. 1b). To corroborate the spatiotemporal profile of the propagating internodal current flow imaged by Diff-CUP, we simulated the same process with the NEURON simulation environment¹⁶. In the reconstructed Diff-CUP movie¹¹, the dynamics of the propagating

internodal current flow in the myelinated axon were consistent with the simulation. To quantify the conduction speed imaged by Diff-CUP, we repeated the imaging experiment under the same conditions using six myelinated axons extracted from four animals. The mean and the standard error of the conduction speeds were 100 m/s and 26 m/s, respectively. Most of the conduction speeds calculated from the Diff-CUP imaging data agreed with the 15–90 m/s speed of APs in 2.5–16 μm myelinated fibers in frogs, but some surpassed this value. Compared to the slow 27 mm/s speed in unmyelinated spiking HEK-293 cells acquired by interferometric imaging⁵ and the 1–7 m/s speed in myelinated L5 pyramidal neurons measured by fluorescence imaging¹³, the 100 m/s averaged speed we measured on myelinated axons with Diff-CUP is the fastest AP-related conduction speed reported using an imaging-based approach.

We also used Diff-CUP to visualize propagations of EMPs through LN. We performed a two-dimensional correlation between adjacent frames and observed the propagation of the EMP as its peak shifted temporally. By linearly fitting the relation between the time shifts of the EMP peaks and the locations of the interference fringes, we calculated the propagation speed of the 150-ps EMP in the LN crystal to be about 5×10^7 m/s. This speed corresponds to a relative permittivity of 36, agreeing with the reported relative permittivity of LN at high frequency, i.e., 25–45¹⁷. To corroborate the dynamics of the propagating EMP acquired by Diff-CUP, we also simulated the electrical field distribution within an LN crystal using an electric field and phase distribution model. Overall, unlike the visualization of electromagnetic waves propagating at a beating frequency implemented with heterodyne or pump-probe approaches, our Diff-CUP system operating in the coded mode enabled the direct visualization of a weak EMP traveling at sub-light speed.

4. CONCLUSION

Enabled by the ultrahigh imaging speed, large sequence depth, and high phase sensitivity, Diff-CUP allows observation of fast internodal current flow propagations, which has not yet been realized, in myelinated axons, as well as sub-light EMP spatiotemporal evolutions in an LN crystal. These are among the fastest biological and physical signals that are rarely investigated. Particularly, the differential approach utilizing alternative stimulations can be immediately applied in other imaging modalities calling for high imaging sensitivity. We envision that, with the capacity to image important biological and physical processes that have not been directly observed before, Diff-CUP opens the door to the investigation of more biological and physical phenomena that are too fast or too weak to be observed using conventional imaging approaches. It can span broad timescales while maintaining high phase sensitivity. Therefore, the technique could find applications in investigating ultrafast biological and physical phenomena.

ACKNOWLEDGEMENTS

This work was supported in part by National Institutes of Health grants R01 NS102213, U01 NS099717, R35 CA220436 (Outstanding Investigator Award), and R01 EB028277. Work in the laboratory of W.G.D. was supported by NIH R01 GM043974.

REFERENCES

- [1] Debanne, D., “Information processing in the axon,” *Nature Reviews Neuroscience* 5(4), 304–316 (2004).
- [2] Hartline, D.K., and Colman, D.R., “Rapid Conduction and the Evolution of Giant Axons and Myelinated Fibers,” *Current Biology* 17(1), R29–R35 (2007).

- [3] Sasagawa, K., Kanno, A., Kawanishi, T., and Tsuchiya, M., “Live electrooptic imaging system based on ultraparallel photonic heterodyne for microwave near-fields,” *IEEE Transactions on Microwave Theory and Techniques* 55(12), 2782–2791 (2007).
- [4] Marquet, P., Depeursinge, C., and Magistretti, P.J., “Review of quantitative phase-digital holographic microscopy: promising novel imaging technique to resolve neuronal network activity and identify cellular biomarkers of psychiatric disorders,” *Neurophotonics* 1(2), 020901 (2014).
- [5] Ling, T., Boyle, K.C., Goetz, G., Zhou, P., Quan, Y., Alfonso, F.S., Huang, T.W., and Palanker, D., “Full-field interferometric imaging of propagating action potentials,” *Light: Science & Applications* 7(1), 107 (2018).
- [6] Kanno, A., Sasagawa, K., Shiozawa, T., and Tsuchiya, M., “Real-time visualization of electromagnetic waves propagating in air using live electro-optic imaging technique,” *Optics Express* 18(10), 10029 (2010).
- [7] Gao, L., Liang, J., Li, C., and Wang, L.V., “Single-shot compressed ultrafast photography at one hundred billion frames per second,” *Nature* 516(7529), 74–77 (2014).
- [8] Liang, J., Ma, C., Zhu, L., Chen, Y., Gao, L., and Wang, L.V., “Single-shot real-time video recording of a photonic Mach cone induced by a scattered light pulse,” *Science Advances* 3(1), e1601814 (2017).
- [9] Wang, P., Liang, J., and Wang, L.V., “Single-shot ultrafast imaging attaining 70 trillion frames per second,” *Nature Communications* 11(1), 2091 (2020).
- [10] Kim, T., Liang, J., Zhu, L., and Wang, L.V., “Picosecond-resolution phase-sensitive imaging of transparent objects in a single shot,” *Science Advances* 6(3), eaay6200 (2020).
- [11] Zhang, Y., Shen, B., Wu, T., Zhao, J., Jing, J.C., Wang, P., Sasaki-Capela, K., Dunphy, W.G., Garrett, D., et al., “Ultrafast and hypersensitive phase imaging of propagating internodal current flows in myelinated axons and electromagnetic pulses in dielectrics,” *Nature Communications* 13(1), 5247 (2022).
- [12] Pezzé, L., and Smerzi, A., “Phase sensitivity of a Mach-Zehnder interferometer,” *Physical Review A* 73(1), 011801 (2006).
- [13] Cohen, C.C.H., Popovic, M.A., Klooster, J., Weil, M.-T., Möbius, W., Nave, K.-A., and Kole, M.H.P., “Saltatory Conduction along Myelinated Axons Involves a Periaxonal Nanocircuit,” *Cell* 180(2), 311-322.e15 (2020).
- [14] Stämpfli, R., and Hille, B., [Electrophysiology of the Peripheral Myelinated Nerve] , in *Frog Neurobiology*, Springer Berlin Heidelberg, Berlin, Heidelberg, 3–32 (1976).
- [15] Brohawn, S.G., Wang, W., Handler, A., Campbell, E.B., Schwarz, J.R., and MacKinnon, R., “The mechanosensitive ion channel TRAAK is localized to the mammalian node of Ranvier,” *eLife* 8, 1–22 (2019).
- [16] Hines, M.L., and Carnevale, N.T., “The NEURON Simulation Environment,” *Neural Computation* 9(6), 1179–1209 (1997).
- [17] Cena, C.R., Behera, A.K., and Behera, B., “Structural, dielectric, and electrical properties of lithium niobate microfibers,” *Journal of Advanced Ceramics* 5(1), 84–92 (2016).